Environmental Modelling & Software 96 (2017) 323–334

Contents lists available at ScienceDirect

Environmental Modelling & Software

journal homepage: www.elsevier.com/locate/envsoft

Fast calculation of groundwater exfiltration salinity in a lowland catchment using a lumped celerity/velocity approach

Joost R. Delsman [a, *], Perry G.B. de Louw [a], Willem J. de Lange [a], Gualbert H.P. Oude Essink [a, b]

[a] Deltares, Unit Subsurface and Groundwater Systems, The Netherlands
[b] Utrecht University, Department of Physical Geography, The Netherlands

ARTICLE INFO

Article history:
Received 9 February 2017
Received in revised form
3 July 2017
Accepted 5 July 2017

Keywords:
Saline groundwater exfiltration
Water quality
Rainwater lens
Shallow groundwater
Model identifiability
Uncertainty evaluation

ABSTRACT

To support operational water management of freshwater resources in coastal lowlands, a need exists for a rapid, well-identifiable model to simulate salinity dynamics of exfiltrating groundwater. This paper presents the lumped Rapid Saline Groundwater Exfiltration Model (RSGEM). RSGEM simulates groundwater exfiltration salinity dynamics as governed by the interplay between water velocity, gradually adjusting the subsurface salinity distribution, and pressure wave celerity, resulting in a fast flow path response to groundwater level changes. RSGEM was applied to a field site in the coastal region of the Netherlands, parameter estimation and uncertainty analysis were performed using generalized likelihood uncertainty estimation. The model showed good correspondence to measured groundwater levels, exfiltration rates and salinity response. Moreover, RSGEM results were very similar to a detailed, complex groundwater flow and transport model previously applied to this field site.

Software availability section

Developed software: RSGEM (Rapid Saline Groundwater Exfiltration Model)
Developer: Joost R. Delsman, Unit Subsurface and Groundwater Systems, Deltares, Utrecht, The Netherlands, P.O. Box 85467, 3508 AL, Utrecht, the Netherlands (joost.delsman@deltares.nl)
First year available: 2015, regular Windows pc, requires python 2.7. Software is freeware, and available from the developer. Program (script) size is 10 kB

1. Introduction

In coastal lowlands, shallow groundwater is often saline as a result of sea water intrusion, past marine transgressions, storm surges or tsunamis, or infiltration from estuarine surface water (McLeod et al., 2010; Post et al., 2013; Werner et al., 2013). The exfiltration of shallow saline groundwater to surface water adversely affects surface water quality and threatens the cultivation of freshwater-dependent crops, drinking water production, industrial use and aquatic ecosystems (Jury and Vaux, 2005). Projected global change foresees a larger demand for freshwater, while the availability decreases due to increasing evapotranspiration, decreasing river runoff, and increasing salinization of groundwater reserves (Ferguson and Gleeson, 2012; Forzieri et al., 2014; IPCC, 2013; Oude Essink et al., 2010; Wada et al., 2013). The increased mismatch between freshwater supply and demand calls for new ways to manage freshwater resources in coastal lowland areas. Successful strategic and operational management of freshwater resources in turn requires improved understanding and modeling of the temporal and spatial dynamics of saline groundwater exfiltration causing surface water salinization.

Where shallow saline groundwater flows upwards, driven by a regional hydraulic gradient, thin rainwater-fed freshwater lenses are often present on top of the saline groundwater (Antonellini et al., 2008; De Louw et al., 2013, 2011a; Delsman et al., 2014b; Vandenbohede et al., 2014; Velstra et al., 2011). A predominantly two-dimensional flow field exists between successive tile drains or ditches (De Louw et al., 2013; Eeman et al., 2011; Maas, 2007). Variations in the thickness of freshwater lenses were shown to be only minor, driven by seasonal variations in precipitation and

* Corresponding author. Unit Subsurface and Groundwater Systems, Deltares, P.O. Box 85467, 3508 AL, Utrecht, The Netherlands.
E-mail address: joost.delsman@deltares.nl (J.R. Delsman).

http://dx.doi.org/10.1016/j.envsoft.2017.07.004

evapotranspiration (De Louw et al., 2013; Eeman et al., 2012), whereas the salinity of groundwater exfiltrating to surface water is highly dynamic and varies on the event scale (De Louw et al., 2013; Delsman et al., 2014b; Velstra et al., 2011). Previous work showed these event-scale salinity dynamics to mainly depend on: (1) clear separation between saline groundwater originating from regional groundwater flow and overlying shallow fresh groundwater of meteoric origin, (2) a fast response of vertical groundwater flux distribution to head variations (pressure wave celerity, cf (McDonnell and Beven, 2014).), resulting in changing contributions of groundwater from different depths and of different salinities, (3) a slower response of groundwater salinity distribution, driven by the low velocity of water droplets, and (4) the possibility of infiltration and subsequent exfiltration of surface water (Delsman et al., 2016, 2014b). Note that buoyancy effects, induced by the density difference between fresh and saline groundwater, appeared negligible compared to occurring hydraulic gradients in a comparable densely-drained lowland catchment (De Louw et al., 2013).

While groundwater flow models have tended to become increasingly complex to represent the heterogeneity in hydrological behavior found on different scales and across catchments (Voss, 2011), the limitations of observational data to adequately identify more complicated model structures and parameters have also become increasingly apparent (Beven, 2006; Delsman et al., 2016; Wagener et al., 2001). Modeling approaches should therefore balance the need for process complexity with the level of complexity supported by the available observational data (Haasnoot et al., 2014; van Turnhout et al., 2016; Wagener et al., 2001). Existing models that simulate the salinity of groundwater exfiltration and resulting surface water salinity encompass a wide range of process complexity. Detailed, spatially distributed (unsaturated) groundwater flow and transport models solve the three-dimensional groundwater flow and advection-dispersion equations, and can represent detailed spatial heterogeneity (Costa et al., 2016; Langevin et al., 2008; Quinn et al., 2004; Therrien et al., 2010). Applications of 2D and 3D distributed models to simulate groundwater exfiltration salinity have been described by (Alaghmand et al., 2016; De Louw et al., 2013; Delsman et al., 2016; Devos et al., 2002). However, these models generally require the estimation of more parameters than can be justified from the available observational data, leaving the inverse problem ill-posed. Furthermore, long run times of such models limit thorough evaluation of model uncertainty (Zhou et al., 2014), and preclude application in operational freshwater management. On the other end of the complexity scale, lumped models as the Sobek-RR model (available from: http://www.deltares.nl/nl/software/108282/sobek-suite) have been used to model exfiltration of salts to surface water (Verhoeven et al., 2013), but the employed fully-mixed conceptualization of the subsurface does not match system understanding (De Louw et al., 2013; Delsman et al., 2016) and will lead to overly smoothed exfiltration salinity dynamics. Recent work on understanding and somehow generalizing the exfiltration of different sources of water within a catchment that together drive solute dynamics, has focused on using (dynamic) travel time distributions as a catchment property (Benettin et al., 2013; Botter et al., 2010; Van der Velde et al., 2012, 2010). However, these approaches only consider solute inputs at the ground surface, and solute dynamics are mainly related to varying inputs driven by recharge variations.

A need therefore still exists for a fast and simple, well-identifiable model structure, that adequately accounts for the main processes governing the salinity dynamics of exfiltrating groundwater. This paper presents Rapid Saline Groundwater Exfiltration Model (RSGEM), a lumped water balance model that simulates groundwater exfiltration salinities based on a celerity/velocity approach. The model aims to include the dominant processes underlying the temporal dynamics of groundwater exfiltration salinity in coastal lowlands. We test the model concept on an agricultural field in the coastal region of the Netherlands, a site where both elaborate field measurements and more detailed modeling approaches are available (Delsman et al., 2016, 2014b). We acknowledge equifinality in model results due to uncertainty in model structure, parameters and observational data (Beven, 2006), and apply the generalized likelihood uncertainty estimation (GLUE) methodology (Beven and Binley, 2013, 1992) to condition model parameters and investigate uncertainty in our model results.

2. Study area and previous modeling

We instrumented a 35 m slice of an agricultural field (Schermerpolder, the Netherlands, 52.599° lat, 4.782° lon) to physically separate and measure different flow routes of water and solute fluxes (Fig. 1). A full description of the field site, measurement setup and measurement results has been presented in (Delsman et al., 2014b), we include only a brief summary here. The subsoil of the instrumented field consists of a consistent 0.2–0.4 m thick tillaged clay layer on top of at least 17 m of fairly homogeneous loamy sand. A system of tile drains (every 5 m, 1 m depth) and ditches drain the average annual precipitation surplus of 290 mm, limiting groundwater level variation to within 0.6 and 1.6 m below ground surface (BGS) (Delsman et al., 2014b). The regional groundwater gradient (De Lange et al., 2014) ensures the upward flow and exfiltration of brackish to saline groundwater (around 5 g/l Cl), originating from marine transgressions around 5000 y. BC (Delsman et al., 2014a; Post et al., 2003). A rainwater lens (De Louw et al., 2011a) overlies the upward flowing brackish groundwater, enabling the cultivation of freshwater-dependent crops on the field.

We separately recorded flow rate and electrical conductivity (EC25) of discharge from tile drains and ditch at 15 min intervals. In- and exfiltration to and from the ditch could not be separately measured, but was calculated using a combined water, salinity and heat balance approach (Delsman et al., 2014b). A station at the agricultural field recorded meteorological information. Groundwater level and EC25 were measured in nine dual piezometers (screened at 0.8–1.0 and 1.8–2.0 m BGS) in a transect perpendicular to the ditch, an additional piezometer screened at 2.8–3.0 m depth was placed in the center of the ditch. We installed soil moisture sensors at different depths both at and between tile drains, and eight temperature sensor arrays in transects both perpendicular and parallel to the ditch-field interface. The groundwater salinity distribution was inferred from geophysical surveys (CVES and EM) before and after the measurement period.

Data was collected during two measurement periods (30 May – 1 Dec 2012 and 15 Apr to – 1 Oct 2013), the field was cultivated and the measurement setup partly dismantled in the intermediate period. Potatoes (planted April 21, 2012, harvested August 20, 2012) were grown on the field in the first period of study, lettuce (planted June 1, 2013, harvested August 9, 2013) was grown in the second. Crop growth was monitored by weekly visual inspection. Actual evapotranspiration was calculated using the FAO Penman-Monteith dual crop-coefficient method (Allen et al., 1998), accounting for the different crops grown (crop factors from Allen et al. (1998)), crop development stages and soil moisture conditions (Delsman et al., 2014b).

Delsman et al. (2016) describe a detailed, distributed, variable-density groundwater flow and transport model of the Schermer field site (Fig. 1c). The model applies SEAWAT (Langevin et al., 2008) and MT3D (Zheng and Wang, 1999; Zheng, 2009) to model temperature-corrected electrical conductivity (EC25) and groundwater temperature respectively for a subsection of the field site, extending from a tile drain to the nearest midpoint between two

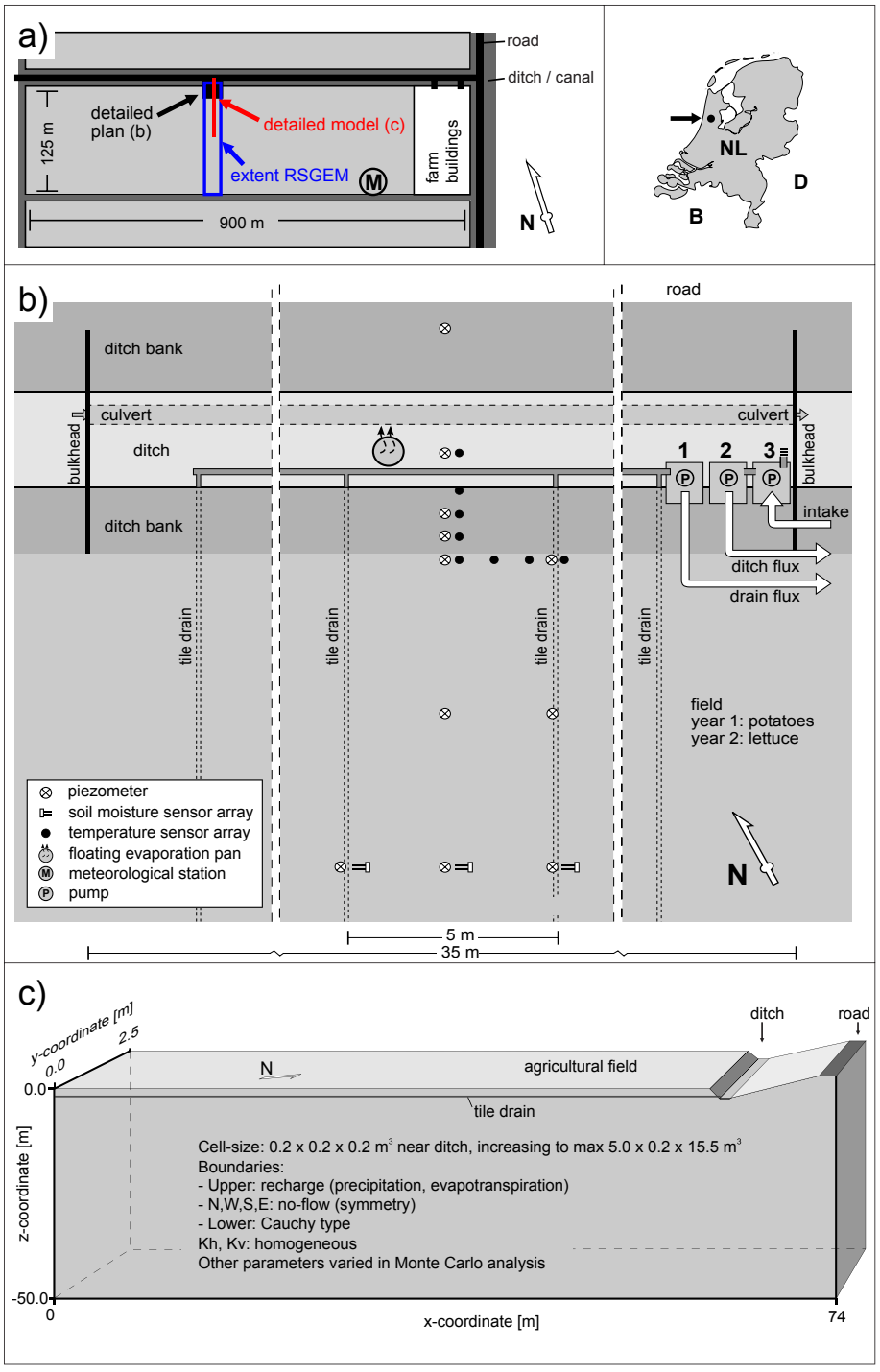

Fig. 1. Location of field site, with overview of field setup and extent of modeling approaches (a), measurement setup around ditch (modified from Delsman et al., 2014b) (b) and conceptual representation of detailed model (modified from Delsman et al., 2016) (c).

tile drains, and from the roadside to the midpoint of the agricultural field (Fig. 1a). The model uses a fine discretization close to the ditch ($0.2 \times 0.2 \times 0.2$ m^3), gradually coarsening away from the ditch to a maximum cell-size of $5.0 \times 0.2 \times 15.5$ m^3. The model was conditioned on different available observational data types using Generalized Likelihood Uncertainty Estimation (GLUE (Beven and Binley, 1992)). A combination of cumulative exfiltration, cumulative salinity load and geophysical measurements of the depth of the fresh – saline interface proved best to constrain uncertainty and capture the relevant processes. The model was subsequently used to investigate exfiltration salinity dynamics at the field site. In this paper, we use this detailed model as an (imperfect) benchmark for RSGEM functioning.

3. Model development

3.1. Model conceptualization

RSGEM (Rapid Saline Groundwater Exfiltration Model) is a lumped water balance model, describing the flow of water and salt

from an agricultural field to surface water, aiming to include the main processes driving the salinity of exfiltrating groundwater as outlined in the introduction. RSGEM simplifies the gradual interface between saline and fresher groundwater (De Louw et al., 2013) to a single, sharp interface. Head variations, driven by recharge and drainage variations, instantaneously affect groundwater flow patterns, and, hence, the distribution of exfiltrated groundwater from above and below the interface. The different contributions of groundwater above and below the interface determine the salinity of exfiltrated groundwater. The fresh – saline interface moves vertically under water balance constraints. Influence of density variations on groundwater flow is considered negligible, given normally occurring pressure gradients and density variations in densely-drained, lowland catchments (De Louw et al., 2013). A conceptual model outline and the model workflow are presented in Fig. 2a and b respectively, a detailed description of the different model steps is presented in the following paragraphs.

3.2. Overall water balance

The water balance for the entire profile, extending from the ground surface to an arbitrary depth can be written as:

$$Sy\frac{dh}{dt} = P - ET + Q_{regional}(h) - Q_{drain}(h) - Q_{ditch}(h), \quad (1)$$

with Sy specific yield, $\frac{dh}{dt}$ head change over time step dt, P precipitation, ET evapotranspiration. Further, $Q_{regional}\ (h)$ is influx of regional groundwater flow, $Q_{drain}\ (h)$ groundwater exfiltration to tile drains and $Q_{ditch}\ (h)$ groundwater exfiltration to the ditch, all a function of head h. Q_{drain} and $Q_{ditch}\ (h)$ are calculated using Eq. (2), see below. RSGEM does not incorporate a description of the unsaturated zone, excluding possible feedbacks between soil moisture and crop transpiration or infiltration rates. We assume the influence of the unsaturated zone on the vertical flow of water to be negligible at the field site, given the shallow water table, excellent water retention characteristics of the soil and the frequent occurrence of macropores at this and similar sites (De Louw et al., 2013; Delsman et al., 2014b; Velstra et al., 2011). Both P and ET are therefore assumed to instantaneously enter or exit the model at groundwater level and must be supplied as time series. As there is no feedback between soil moisture and ET, possible reduction of evapotranspiration due to soil moisture limitations must be accounted for prior to running RSGEM.

$Q_{regional}$, the influx of regional groundwater flow, is implemented as a linear Cauchy-type boundary condition, and requires providing the model with both a time series of heads in an underlying aquifer, and a hydraulic resistance between the aquifer and the arbitrary model domain. Alternatively, a time series of the regional groundwater flux may be provided, e.g. derived from large-scale groundwater models.

Exfiltration of groundwater to tile drains and ditches is calculated using the classic Hooghoudt equation (Hooghoudt, 1940), using the approximation by Moody (1966) to account for radial flow.

$$q = \begin{cases} \dfrac{8KD_{eff}m_0 + 4Km_0^2}{L^2}, & \text{if } m_0 \geq 0 \\ \dfrac{8KD_{eff}m_0 - 4Km_0^2}{L^2}, & \text{if } m_0 < 0 \end{cases}, \quad (2)$$

in which q is specific discharge, the flux between groundwater and surface water (m/d), K is the hydraulic conductivity (m/d), D_{eff} is the effective depth of flow (the total flow depth corrected to account for radial flow, calculated using (Moody, 1966)), m_0 is the groundwater level above drainage level at $0.5L$, and L is the distance between drains (Hooghoudt, 1940). The Hooghoudt equations for groundwater exfiltration to tile drains and ditches ($m_0 > 0$), and infiltration from ditches ($m_0 < 0$) assumes stationary flow, bounded at the bottom by an aquiclude, and at the top by a curved phreatic surface. The left and right parts in the numerator represent flow between

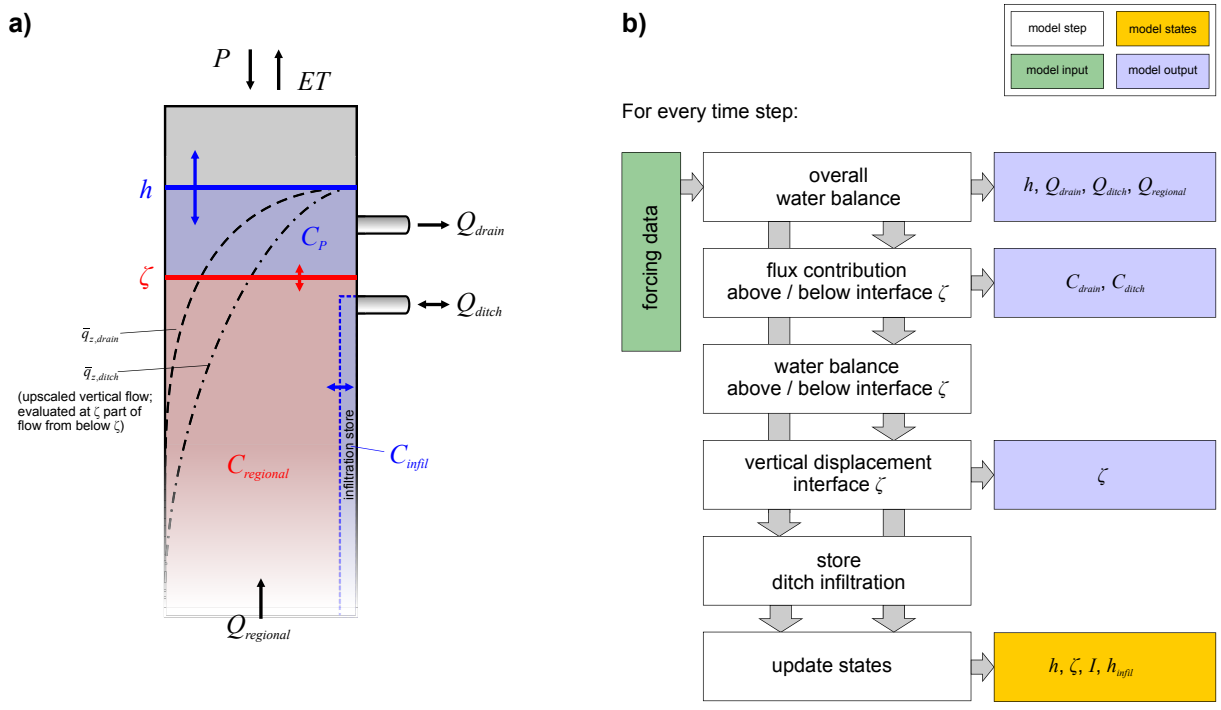

Fig. 2. a) Conceptual outline of RSGEM, b) RSGEM workflow; symbols are listed in Table 1.

this aquiclude and the drainage level, and flow between the drainage level and the curved phreatic surface respectively. Note that we assume a single K, instead of different Ks above and below the drainage level as in Hooghoudt's (1940) original formulation. Anisotropy was accounted for by replacing K with the equivalent $\sqrt{K_v K_h}$, L with $L\sqrt{K_v/K_h}$, and q with $q/\sqrt{K_v K_h}$ (Smedema et al., 1985), in which K_h is horizontal, and K_v is vertical hydraulic conductivity. The drainage level of tile drains is calculated as the maximum of the elevation of the drains and water level in the ditch, as the collector drain (effectively the drainage base for the tile drains) could float upward when ditch water levels were high.

3.3. Fresh – saline interface dynamics

RSGEM assumes a sharp interface between shallow fresh groundwater of meteoric origin, and deeper saline groundwater that originated from regional groundwater flow. RSGEM tracks the movement of this interface by considering separate water balances above and below the fresh – saline interface. Recalling that P and ET enter and exit the model at groundwater level, the water balance above the interface reads:

$$-\eta\frac{d\zeta}{dt} = P - ET - Q_{drain,above} - Q_{ditch,above} - Sy\frac{dh}{dt}, \tag{3}$$

in which η is effective porosity, $\frac{d\zeta}{dt}$ is the vertical movement of the fresh – saline interface ζ over time step dt, positive directed upwards, $Q_{drain,\ above}$ is the proportion of tile drain exfiltration that originates above the fresh – saline interface, $Q_{ditch,\ above}$ is likewise the proportion of ditch exfiltration originating above the interface. The water balance below the interface, with $Q_{regional}$ entering the model from below, reads:

$$\eta\frac{d\zeta}{dt} = Q_{regional} - Q_{drain,below} - Q_{ditch,below}, \tag{4}$$

where $Q_{drain,\ below}$ and $Q_{ditch,\ below}$ are the respective proportions of Q_{drain} and Q_{ditch} that originate below the fresh – saline interface.

This approach, however, leaves the question of how to separate the proportions of Q_{drain} and Q_{ditch} originating above and below the fresh – saline interface. Groenendijk and Van den Eertwegh (2004) present a derivation of a one-dimensional vertical projection of the two-dimensional groundwater flow field typical of flow to lowland tile drains. They extend the work of Ernst (1973), who presented a complex potential function for two-dimensional groundwater flow in an infinitely deep, homogeneous aquifer receiving only recharge at the ground surface, and exfiltrating at a shallow drain at $\frac{L}{2}$ (Fig. 3a). They then consider each streamline to represent a certain portion of total groundwater flow. They posit that each streamline, flowing from the surface downwards and upwards towards a tile drain or ditch, has a deepest point and, hence, the deepest point of each streamline represents the vertical limit of a certain portion of the total flow. They go on to define the "upscaled vertical flux" $\overline{q}_z$ as the flow (or recharge) that still crosses a given depth and flows downward. Groenendijk and Van den Eertwegh (2004) derive the following function for $\overline{q}_z$:

$$\overline{q}_z(z) = R\frac{2}{\pi}\arctan\left(\frac{\exp\left(\frac{2\pi z}{L}\right)}{\sqrt{1-\exp\left(\frac{4\pi z}{L}\right)}}\right), \tag{5}$$

with the upscaled vertical flux at depth z and R being recharge. The upscaled vertical flux from Eq. (5) is R at groundwater level, and exponentially decreases downward (Fig. 3b). Eq. (5) obviously oversimplifies occurring groundwater flow patterns, given for instance heterogeneity in the subsurface and superimposed regional groundwater flow, but provides a first order estimate of the vertical distribution of groundwater flow. Also note that the derived Eq. (5) is specific to the considered hydrogeologic problem: an homogeneous aquifer where drain spacing is small relative to the aquifer depth; different physiographic situations may require a different formulation for the upscaled vertical flux $\overline{q}_z$ (Groenendijk and Van den Eertwegh, 2004). The described method was devised for and is implemented in the Richards-type SWAP and associated nutrient transport ANIMO models (Groenendijk et al., 2005; Kroes et al., 2008; van Dam et al., 2008), although these apply a different formulation for the upscaled vertical flux, assuming fully penetrating drains and thus negligible radial flow.

Evidently, $R - \overline{q}_z(z)$ then gives the flow that does not cross a given depth, but exfiltrates to a tile drain or ditch without having passed deeper through the subsurface. In the following, we use this formulation to obtain the contributions of flow to tile drains and ditches above and below the fresh – saline interface. We apply Eq. (5) with the flow to tile drains or ditches (Q_{drain}, Q_{ditch}) instead of R, and account for anisotropy by replacing L with $L\sqrt{K_v/K_h}$. Solving at the fresh – saline interface ($z = \zeta$) for the flux to tile drains and the flux to ditches then gives the respective flux proportions above ($Q_{drain,\ above}$, $Q_{ditch,\ above}$) and below ($Q_{drain,\ below}$, $Q_{ditch,\ below}$) the fresh – saline interface, for subsequent substitution in Eqs (3) and (4):

$$Q_{i,above} = Q_i\left(1 - \frac{2}{\pi}\arctan\left(\frac{\exp\left(\frac{2\pi\zeta}{L_i\sqrt{K_h K_v}}\right)}{\sqrt{1-\exp\left(\frac{4\pi\zeta}{L_i\sqrt{K_h K_v}}\right)}}\right)\right), \tag{6}$$

$$Q_{i,below} = Q_i\frac{2}{\pi}\arctan\left(\frac{\exp\left(\frac{2\pi\zeta}{L_i\sqrt{K_h K_v}}\right)}{\sqrt{1-\exp\left(\frac{4\pi\zeta}{L_i\sqrt{K_h K_v}}\right)}}\right), \tag{7}$$

with i denoting either drain or ditch. RSGEM neglects specific storativity (water and soil are considered incompressible) in the saturated zone; adjustment of the flow pattern to head variations is therefore instantaneous. Note that the fresh – saline interface can, by definition, never exceed the groundwater level.

3.4. Exfiltration salinity

The variation of the salinity of regional groundwater flow and precipitation over the timescales considered was found to be negligible at the field site (Delsman et al., 2014b) and in similar settings (De Louw et al., 2013). RSGEM therefore applies a constant flow route concentration approach (as, e.g., De Louw et al., 2011b; Iorgulescu et al., 2005), which calculates groundwater exfiltration salinity as the flux-weighted average of the different constituting flow route salinities:

$$\begin{aligned} C_{drain} &= \frac{C_P Q_{drain,above} + C_{regional} Q_{drain,below}}{Q_{drain}} \\ C_{ditch} &= \frac{C_P Q_{ditch,above} + C_{regional} Q_{ditch,below} + C_{infil} Q_{ditch,infil}}{Q_{ditch}}, \end{aligned} \tag{8}$$

in which C_{drain} is the salinity of drain exfiltration, C_{ditch} is the salinity

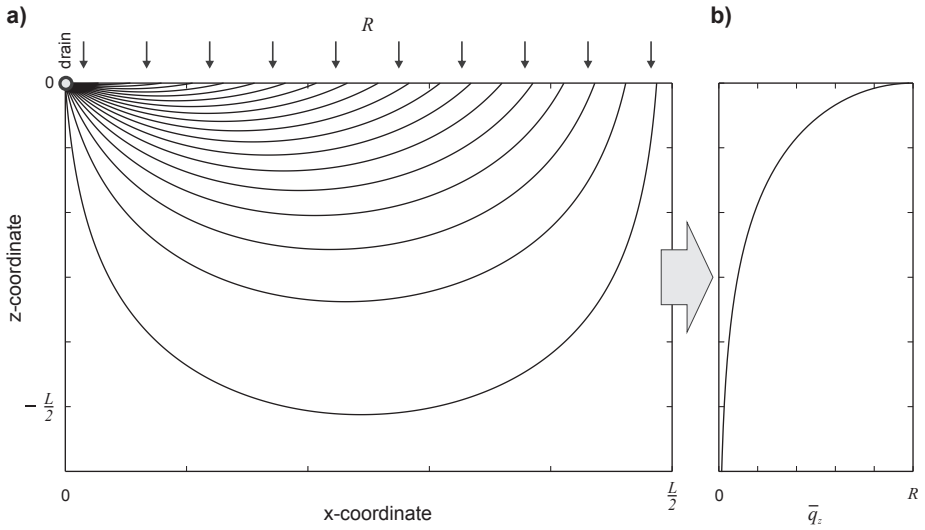

Fig. 3. Streamfunction of flow of recharge R towards a drain in an infinitely deep, homogeneous aquifer (a), and corresponding upscaled vertical flux $\bar{q}_z$ with depth according to Eq. (5) (b) (after Groenendijk and Van den Eertwegh (2004)).

of ditch exfiltration, C_P is the salinity of precipitation, $C_{regional}$ the salinity of regional groundwater flow, C_{infil} is the salinity of infiltrated surface water, and $Q_{ditch,\ infil}$ is the part of Q_{ditch} that originated as surface water infiltration.

3.5. Infiltration and exfiltration of surface water

Infiltration of surface water is only possible from the ditch, not from tile drains. The amount of infiltrated surface water, the infiltration store, is tracked in the model. Additionally, RSGEM calculates and retains the flux-averaged infiltration surface water level, or infiltration level, to keep track of the vertical extent of infiltrated water in the model column. The store of infiltrated water is emptied when the system reverts to a draining state. The outflow of previously infiltrated water is calculated by evaluating Eq. (5) at the saved infiltration level, to obtain the fraction of Q_{ditch} transporting previously infiltrated water to the ditch. Innate water below the infiltration level only exfiltrates when the infiltration store has been depleted. Exfiltration fluxes above the infiltration level are unaffected by previous infiltration.

3.6. Model implementation

RSGEM is implemented in the Python 2.7 programming language; model code is available from the first author. Equations are solved explicitely from the previous state, the water balance (Eqs. (1) and (2)) is solved iteratively. The model keeps 4 state variables as a function of time (groundwater level, interface depth, infiltration amount and infiltration level), and requires 17 parameters (Table 1), for 4 of which (K_h, K_v, η, Sy) parameter estimation is advised. Other parameters can be derived relatively straightforwardly from field measurements. Model execution time averages 14 s for 12500 time steps on a single Intel i5 2.8 GHz processor. RSGEM can be used stand-alone, or provide fluxes of water and salt to a hydrodynamic model.

4. Model application

4.1. Generalized likelihood uncertainty estimation

We estimated model parameters and evaluated the uncertainty in our modeling approach by applying the generalized likelihood uncertainty evaluation (GLUE) methodology of Beven and Binley (1992). Given unavoidable (and often epistemic rather than random) errors in model structure, model parameterization, and observational data, GLUE recognizes that multiple models will be equally good descriptors of reality and thus exhibit equifinality (Beven, 2006). GLUE retains multiple model structures or model parameterizations that are considered behavioral given some (subjective) adequate fit to available measurement data. Results of all behavioral models are then weighted according to a likelihood measure (be it formal, informal or fuzzy), expressing a degree of confidence in the model. GLUE implicitly accounts for model structural error and hence does not require possibly wrong assumptions on the model error structure (Beven, 2009). The prior collection of models is generally obtained by uniform Monte Carlo sampling of parameter ranges, although more advanced Markov Chain Monte Carlo methods have also been used (e.g., Blasone et al., 2008; Rojas et al., 2010). Despite being criticized for lacking the objectivity of formal Bayesian approaches (Clark et al., 2011; Mantovan and Todini, 2006; Stedinger et al., 2008), the GLUE methodology has found widespread use in the hydrological modeling community (Beven and Binley, 2013). For a more complete description of GLUE, the reader is referred to (Beven and Binley, 1992; Beven, 2009, 2006).

4.2. Application to the schermer field site

We applied RSGEM to the Schermer field site and set most parameters to measured values (Table 1). We used a spin-up time of five years, ensuring the establishment of the fresh – saline interface depth, preceding the May 1, 2012–October 1, 2013 model period. We applied daily time steps during spin-up, and hourly time steps during the model period. Forcing data for the spin-up period was obtained from nearby meteorological stations operated by the Royal Netherlands Meteorological Institute, forcing data for the analyzed period was measured by the local meteorological station. Actual evapotranspiration (ET) was calculated using the FAO Penman-Monteith dual crop-coefficient method, with growing stages based on weekly visual observations, and potential evapotranspiration corrected to actual using shallow soil moisture data (Delsman et al., 2014b). Differences in crop characteristics (potatoes

and lettuce in the first and second year of study respectively) were accounted for in the calculation. Evapotranspiration was additionally multiplied by a single evapotranspiration factor, to account for uncertainties in evapotranspiration estimates. The evapotranspiration factor was varied between 0.5 and 1.5 in the uncertainty analysis (Table 2). Heads at the lower boundary were obtained from a representative piezometer 500 m to the northwest of the field site. For field conditions at the Schermer polder, temperature-corrected electrical conductivity (EC25) of groundwater may be assumed to behave conservatively and mix linearly, as chloride is by far the dominant anion contributing to EC25 (Delsman et al., 2014b). We therefore used EC25 as the modeled solute, and assigned measured EC of deep groundwater (21.8 mS/cm), shallow groundwater (1.0 mS/cm) and ditch water (2.0 mS/cm) during infiltration periods to the concentration of deep groundwater ($C_{regional}$), precipitation (C_P) and infiltration (C_{infil}) respectively. Observed ditch water EC25 was relatively constant during infiltration periods, justifying the applied constant value. We used EC25 of shallow groundwater rather than precipitation EC25, to account for admixing of solutes stored in the soil.

4.3. Parameter estimation and likelihood measure

We considered hydraulic conductivity, effective porosity, specific yield, anisotropy, hydraulic resistance lower boundary, and evapotranspiration factor in parameter estimation. We uniformly sampled these six model parameters to obtain $1{\cdot}10^5$ parameter sets, using a Latin Hypercube sampler (LHS). LHS is more efficient in representatively sampling the entire parameter space than ordinary random sampling, and has been shown to only require about 10% of samples compared to ordinary sampling to obtain representative uncertainty estimates (Yu et al., 2001). Model parameters were sampled either in normal or in log-space; ranges were derived either from field measurements (range extended to allow for measurement error), or were based on literature ranges (sampled ranges in Table 2).

We evaluated the RSGEM model jointly on the simulated groundwater level, tile drain exfiltration, ditch in-/exfiltration, cumulatives of the latter two, tile drain exfiltration salinity, ditch exfiltration salinity, and cumulative loads of both tile drains and ditch. We used the following likelihood measure that evaluates all observation types:

$$L(O|\theta_i) = \sum_{j=1}^{m} \frac{W_j}{\sigma^2_{i,j}} \Big/ C, \tag{9}$$

With $L(O|\theta_i)$ the likelihood of parameter set θ of the ith model, given observations O, $\sigma^2_{i,j}$ the mean squared error of the ith model for j of m observation types, W_j the weight assigned to observation type j, C is a scaling constant to sum behavioral likelihoods to one. We assigned weights based on the inverse of the interquartile range of calculated mean squared errors. We used a relative limit of acceptability approach and considered the top 1% runs behavioral, discarding the remaining 99% from further analysis.

Table 1
RSGEM parameters, states and boundary conditions, and values used in Schermer field site application.

Parameter	Symbol	Unit	Schermer value[a]
Hydraulic conductivity	K	m/d	Estimated
Effective porosity	η	–	Estimated
Specific yield	Sy	–	Estimated
Anisotropy	Kh/Kv	–	Estimated
Drain level	h_{drain}	m	−1.
Drain distance	L_{drain}	m	5.
Drain width	b_{drain}	m	0.1
Ditch water level	h_{ditch}	m	−1.06; time series
Ditch bottom	bot_{ditch}	m	−1.3
Ditch distance	L_{ditch}	m	125.
Ditch width	b_{ditch}	m	2.
Ditch infiltration possible	inf_{ditch}	–	False; True
Hydraulic resistance lower boundary	c_{lbc}	d	Estimated
Concentration recharge	C_P	mS/cm	1.
Concentration regional groundwater	$C_{regional}$	mS/cm	21.8
Concentration infiltration	C_{infil}	mS/cm	2.
Time step	t	s	86400.; 3600.
State	Symbol	Unit	Schermer start
Groundwater level	h	m	−1.
Interface level	ζ	m	−1.5
Infiltration	I	mm	0
Infiltration level	h_{infil}	m	−1.
Boundary condition/forcing	Symbol	Unit	
Precipitation	P	mm/d	
Actual evapotranspiration	ET	mm/d	
Head lower aquifer	$h_{regional}$	m	
Regional groundwater flux	$Q_{regional}$	mm/d	
Model output	Symbol	Unit	
Exfiltration to tile drains	Q_{drain}	mm/d	
Ex-/infiltration to/from ditch	Q_{ditch}	mm/d	
Concentration drain exfiltration	C_{drain}	mS/cm	
Concentration ditch exfiltration	C_{ditch}	mS/cm	

[a] When two values are given, they correspond to the spin-up and calculation periods respectively.

Table 2
A priori ranges of estimated RSGEM parameters.

Parameter	Range	Normal or log space
Hydraulic conductivity	0.005–50.	Log
Effective porosity	0.1–0.6	Normal
Specific yield	0.01–0.3	Normal
Anisotropy	0.5–20.	Log
Hydraulic resistance lower boundary	100–10000	Log
EVT factor[a]	0.5–1.5	Normal

[a] EVT factor is not a true RSGEM parameter, but a factor applied to actual evapotranspiration time series prior to each model run.

5. Results

The top 1% of $1{\cdot}10^5$ runs corresponded to 1000 behavioral runs. Dotty plots of behavioral parameter distributions are shown in Fig. 4. Parameters K (hydraulic conductivity) and C_{lbc} (hydraulic resistance lower boundary) showed clear conditioning: behavioral parameters were constrained to a well-defined region within the defined a priori ranges. Sy (specific yield) and f_{EVT} (evapotranspiration factor) are conditioned to a lesser extent. Parameters K_h/K_v (anisotropy) and η (effective porosity) show no clear conditioning. Constrained values of parameter K (around 0.05 m/d) compare well to field measurements (Delsman et al., 2014b). Parameters C_{lbc} en Sy are constrained to values comparable to calibrated parameters for the detailed model of the field site (Delsman et al., 2016). Hydraulic conductivity K, while corresponding to field measurements, is constrained to an order of magnitude lower than values resulting from parameter estimation of the detailed model. This could result from K encompassing the hydraulic resistance of the porous matrix as well as the entry resistance of drains and ditch, in both RSGEM and field slug tests, while the two components are separated in the detailed model.

Time series of modeled groundwater level, tile drain and ditch exfiltration and salinities generally showed good correspondence to measured values (Fig. 5). Head dynamics and tile drain exfiltration were modeled well, except for the May–July 2013 period, when the relatively constant measured groundwater level and exfiltration were not matched by the model (Fig. 5b,d). For instance,

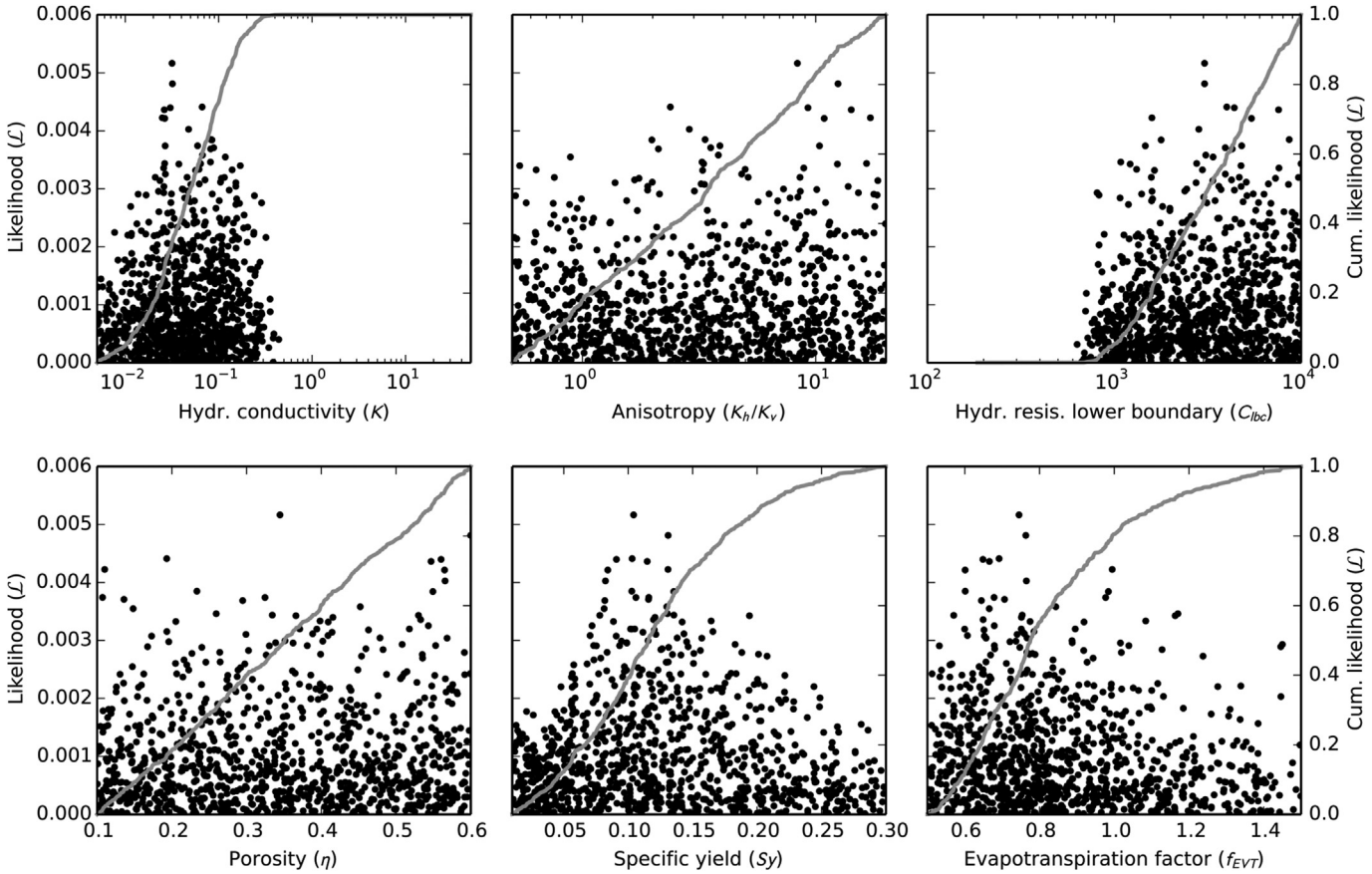

Fig. 4. Dotty plots of behavioral parameter values (black dots), overlain by cumulative distribution function (gray line).

between June 1 and June 20, 2013, RSGEM simulated falling groundwater levels not reflected in the measurements and hence could not reproduce the tile drain exfiltration peak around June 20, 2013. This model behavior may result from not incorporating the unsaturated zone and crop response in RSGEM; groundwater levels could therefore not be sustained by release of water from storage in the unsaturated zone, or by reduced actual evapotranspiration rates. Model performance is restored in July 2013, when the system further dries out and groundwater levels drop both in RSGEM and the measurements. While its dynamics were captured well, ditch exfiltration was somewhat overestimated by the model. This overestimation could partly result from incommensurability between the modeled and measured ditch exfiltration. The fixed factor we applied to correct for differences in catchment area (RSGEM: entire width of agricultural field, measurements: half the agricultural field, plus other side of ditch to road) did not account for differences in flow between the agricultural field and the other side of the ditch. Ditch infiltration rates in August 2013 were, however, captured well (Fig. 5f). Salinity dynamics of tile drain exfiltration were well reproduced by the model, again except for the May–July 2013 period (Fig. 5e). The underestimation of groundwater levels and tile drain exfiltration during this period led to an overestimation of tile drain exfiltration salinity, as deeper flowpaths were predicted than actually occurred. Dynamics of ditch exfiltration salinity were reproduced well by the model, including the low exfiltration salinity after the August 2013 infiltration period (Fig. 5g). The modeled fresh – saline interface (Fig. 5c) was the most uncertain model output, as it was not constrained directly by including the depth of the fresh – saline interface in the likelihood calculation. The influence of the fresh – saline interface depth on exfiltration salinity dynamics apparently was not enough to better constrain the depth of the interface.

We also compared RSGEM results to results of the detailed model of the field site. RSGEM results were generally very comparable to modeled timeseries from the detailed model (Fig. 6). Notably, the calculation of the tile drain salinity, accounting for around 80% of the salt load to surface water (Delsman et al., 2014b) and hence one of the most important model results, is very comparable between the two models. The detailed model was equally unable to match the measured sustained groundwater levels in the May–July 2013 period; likely also resulting from not incorporating the unsaturated zone in the detailed model. Measured ditch exfiltration was better reproduced by the detailed model than by RSGEM; contrary to RSGEM, the detailed model includes the other side of the ditch and thus spans the exact catchment area of the ditch. Neither model could well represent the salinity of ditch exfiltration. However, the almost binary (either fresh or saline) measured response of ditch exfiltration salinity was better matched by RSGEM, than by the detailed model. The RSGEM-modeled depth of the fresh – saline interface corresponded well to the depth of the fresh – saline interface calculated by the detailed model, both in absolute depth and variation over the model period.

6. Discussion

Modeling approaches balance the need for process complexity with the need for identifiability of the model structure from the available observational data (van Turnhout et al., 2016; Wagener et al., 2001). This paper presents RSGEM (Rapid Saline Groundwater Exfiltration Model), a model that simulates dynamics of the

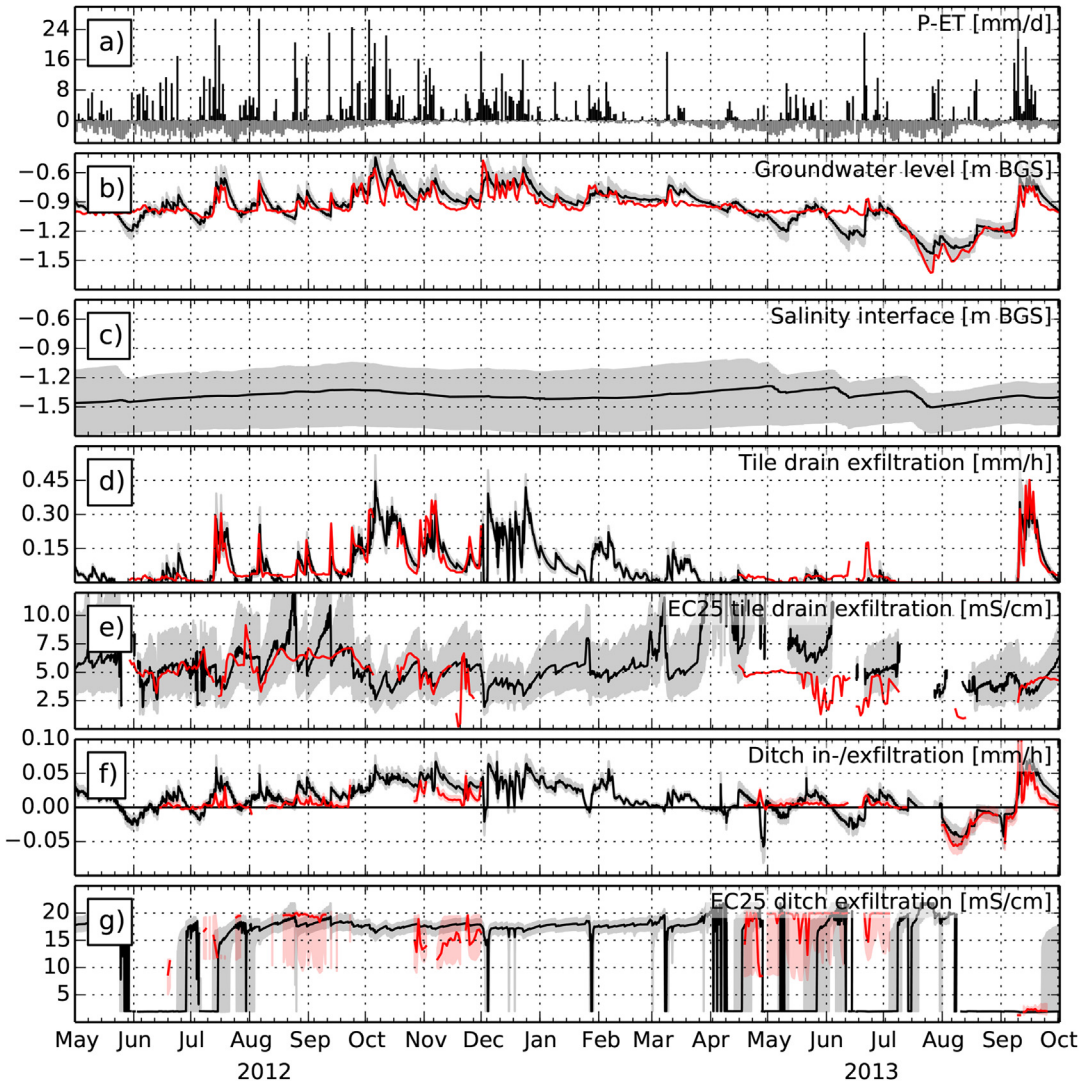

Fig. 5. Measured precipitation (black bars) and calculated actual evapotranspiration (gray bars) (a), groundwater level (b), fresh − saline interface level (c), tile drain exfiltration (d), EC25 of tile drain exfiltration (e), ditch in- and exfiltration (f), and EC25 of ditch exfiltration (g). Red lines denote measured values, black lines denote median model results, and gray shaded area denotes 25–75 percentile of model results. Shaded red areas around measured values in f) and g) are the 25–75% percentiles of Monte Carlo uncertainty estimates (Delsman et al., 2014b). (For interpretation of the references to colour in this figure legend, the reader is referred to the web version of this article.)

groundwater fresh − saline interface and groundwater exfiltration salinity in lowland coastal catchments using a simple, lumped model structure. Following a recent appeal for understanding the interplay between water velocity and wave celerity (McDonnell and Beven, 2014), the basis of the model is formed by the recognition that groundwater exfiltration salinity dynamics are driven by both pressure wave celerity and water velocity. The fast responding pressure distribution (instantaneous in RSGEM, as we assume incompressible water and no unsaturated zone) has an immediate impact on flow patterns, discharging water from above or below a defined interface in groundwater salinity. This interface itself reacts subdued, driven by the actual vertical flow of water droplets. In lowland areas where diverted river water is used to supplement precipitation deficits, the possible infiltration and subsequent exfiltration of surface water represents an additional important control on exfiltration salinity dynamics (Delsman et al., 2016, 2014b). Application of the presented model is foreseen in simulating surface water salinization, evaluating possible measures mitigating surface water salinization, and forecasting and managing surface water salinization in an operational setting.

Short model run times allowed for an elaborate evaluation of the uncertainty in six model parameters using the GLUE methodology (Beven and Binley, 1992). Constrained model parameters were consistent with field measurements or constrained parameters from a detailed model of the studied field site, establishing confidence in the physical basis of the model. Moreover, constrained model results showed good correspondence with measured groundwater levels, values of different flow route contributions to surface water and their associated salinities. Clear similarity of modeled RSGEM responses and results from the detailed model, including similar deficiencies during the May–July 2013 period, further showed the ability of the lumped RSGEM concept to capture the dominant processes driving salinity dynamics in exfiltrating groundwater. So, while the presented lumped approach is evidently a simplification of the 2D or even 3D, transient and heterogeneous processes occurring in the subsurface, relatively good correspondence to not only measured groundwater levels, but also exfiltration rates and their chemical response points towards "getting the right answers for the right reasons" (Kirchner, 2006). Further research and applications in different physiographic

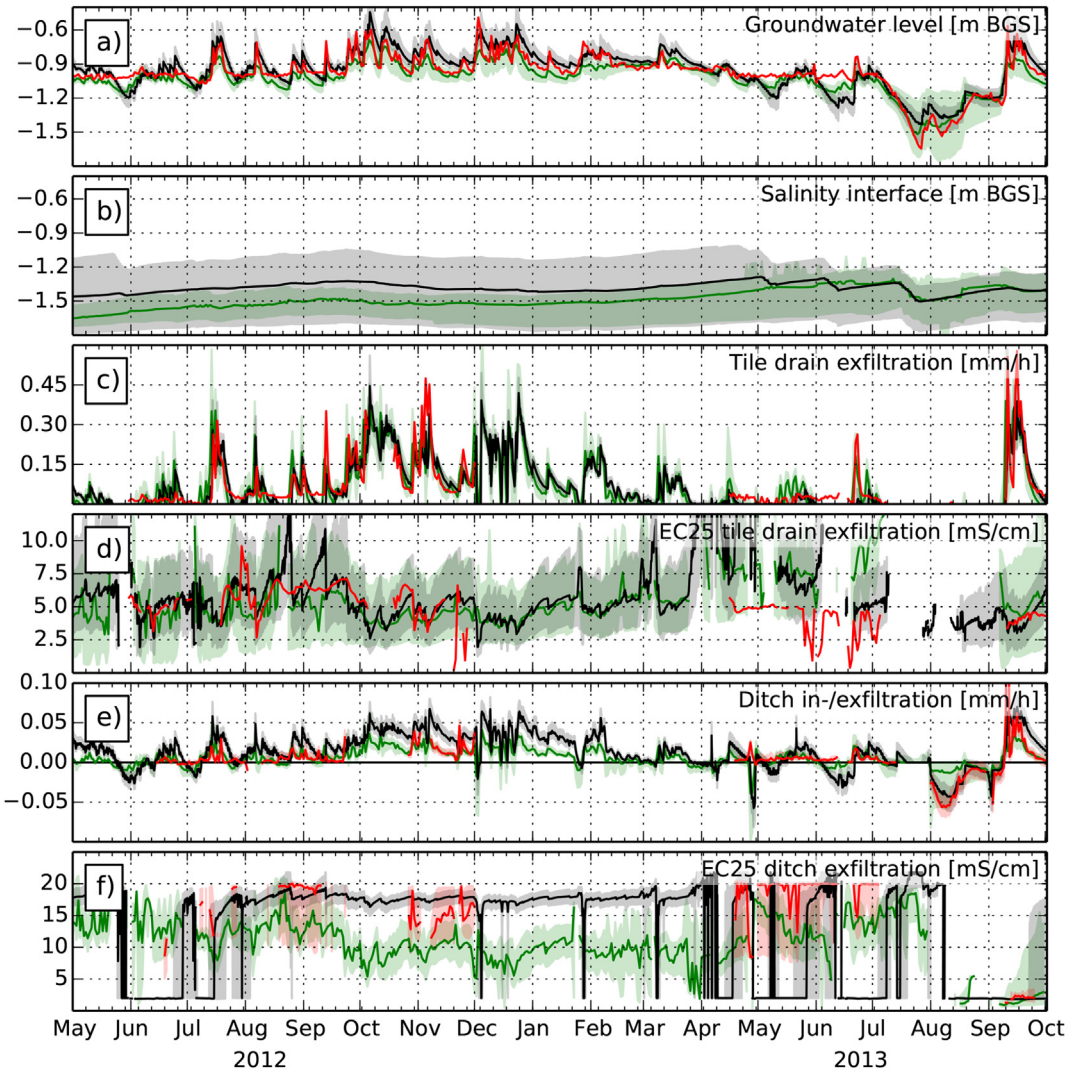

Fig. 6. Comparison of groundwater level (a), fresh − saline interface level (b), tile drain exfiltration (c), EC25 of tile drain exfiltration (d), ditch in- and exfiltration (e), and EC25 of ditch exfiltration (f) between RSGEM and detailed model. Black lines denote median RSGEM results, green lines median detailed model results. Gray and green shaded areas denotes 25–75 percentile of RSGEM and detailed model results, respectively. Red lines denote measurements, shaded red areas around measured values in e) and f) are the 25–75% percentiles of Monte Carlo uncertainty estimates (Delsman et al., 2014b). (For interpretation of the references to colour in this figure legend, the reader is referred to the web version of this article.)

settings must, however, precede more definitive trust in the proposed model structure.

Central to the calculation of groundwater exfiltration salinity in RSGEM is the division of fluxes between originating from above or below the fresh − saline interface (Eq. (5)). While the proposed exponential decrease results in realistic salinity dynamics in this particular case, flow fields in other settings may be better approximated by different functions. Other settings may include different drainage characteristics, more prominent density contrasts between deep and shallow groundwater, or with strongly heterogeneous aquifers. Analytical functions of 2D flow fields are available for a range of different hydrogeologic problems (e.g., Bruggeman, 1999; Ernst, 1973), and may be used to derive exfiltration-attribution-functions similar to Eq. (5). Alternatively, detailed numerical models could be used to derive such functions. A third possibility may be provided by recent work on using dynamic travel time distributions as a catchment property (Benettin et al., 2013; Botter et al., 2010; Van der Velde et al., 2012, 2010). Although not directly applicable, as salinity dynamics are not driven by temporal variations in surface inputs, catchment-averaged travel time distributions (or storage outflow probability functions (Van der Velde et al., 2012)) may also offer a way of modeling 'which water is discharged'. Further work is needed to delineate appropriate application ranges for the current (Eq. (5)) and explore other possible exfiltration-attribution-functions.

Although influence of the unsaturated zone on the hydrologic response of the field site was minimal during most of the model period, measured groundwater levels appeared to be sustained during dry periods by either a slow depletion of water stored in the unsaturated zone or an unaccounted for decrease in actual evapotranspiration (e.g., May–July 2013). Adding a parsimonious conceptualization of the unsaturated zone and crop response to the model structure will likely improve model performance during such dry periods. Furthermore, addition of the unsaturated zone will extend the applicability of RSGEM to settings with a more dominant role of the unsaturated zone in their hydrologic functioning. As an alternative, the RSGEM methodology to calculate salinity dynamics could also easily be included in other lumped rainfall-runoff approaches (e.g., the recently developed WALRUS model for similar lowland settings (Brauer et al., 2014)).

Acknowledgements

We thank Boran Aydin and Ilmar Kelderman for user feedback on the application of RSGEM. A draft version of this paper is included in the PhD thesis of the corresponding author and has been published as such (Delsman, 2015).

References

Alaghmand, S., Beecham, S., Woods, J.A., Holland, K.L., Jolly, I.D., Hassanli, A., Nouri, H., 2016. Quantifying the impacts of artificial flooding as a salt interception measure on a river-floodplain interaction in a semi-arid saline floodplain. Environ. Model. Softw. 79, 167–183.

Allen, R., Pereira, L., Raes, D., Smith, M., 1998. Crop Evapotranspiration-Guidelines for Computing Crop Water Requirements-FAO Irrigation and Drainage Paper 56. FAO, Rome, Rome, Italy.

Antonellini, M., Mollema, P., Giambastiani, B.M.S., Bishop, K., Caruso, L., Minchio, a., Pellegrini, L., Sabia, M., Ulazzi, E., Gabbianelli, G., 2008. Salt water intrusion in the coastal aquifer of the southern Po Plain, Italy. Hydrogeol. J. 16, 1541–1556.

Benettin, P., Van der Velde, Y., Van der Zee, S.E.A.T.M., Rinaldo, A., Botter, G., 2013. Chloride circulation in a lowland catchment and the formulation of transport by travel time distributions. Water Resour. Res. 49, 4619–4632.

Beven, K.J., 2006. A manifesto for the equifinality thesis. J. Hydrol. 320, 18–36.

Beven, K.J., 2009. Environmental Modelling: an Uncertain Future? Routledge/Taylor & Francis, London.

Beven, K.J., Binley, A.M., 1992. The future of distributed models: model calibration and uncertainty prediction. Hydrol. Process 6, 279–298.

Beven, K., Binley, A., 2014. GLUE: 20 years on. Hydrol. Process 28 (24), 5897–5918. http://dx.doi.org/10.1002/hyp.10082.

Blasone, R.-S., Vrugt, J.A., Madsen, H., Rosbjerg, D., Robinson, B.A., Zyvoloski, G.A., 2008. Generalized likelihood uncertainty estimation (GLUE) using adaptive Markov Chain Monte Carlo sampling. Adv. Water Resour. 31, 630–648.

Botter, G., Bertuzzo, E., Rinaldo, A., 2010. Transport in the hydrologic response: travel time distributions, soil moisture dynamics, and the old water paradox. Water Resour. Res. 46, 1–18.

Brauer, C.C., Teuling, A.J., Torfs, P.J.J.F., Uijlenhoet, R., 2014. The Wageningen Lowland Runoff Simulator (WALRUS): a lumped rainfall–runoff model for catchments with shallow groundwater. Geosci. Model Dev. Discuss. 7, 1357–1411.

Bruggeman, G.A., 1999. Analytical Solutions of Geohydrological Problems, Developments in Water Science. Elsevier, Amsterdam.

Clark, M.P., Kavetski, D., Fenicia, F., 2011. Pursuing the method of multiple working hypotheses for hydrological modeling. Water Resour. Res. 47, 1–16.

Costa, D., Burlando, P., Liong, S.Y., 2016. Coupling spatially distributed river and groundwater transport models to investigate contaminant dynamics at river corridor scales. Environ. Model. Softw. 86, 91–110.

De Lange, W.J., Prinsen, G.F., Hoogewoud, J.C., Veldhuizen, A.A., Verkaik, J., Oude Essink, G.H.P., Van Walsum, P.E.V., Delsman, J.R., Hunink, J.C., Massop, H.T.L., Kroon, T., 2014. An operational, multi-scale, multi-model system for consensus-based, integrated water management and policy analysis: The Netherlands hydrological instrument. Environ. Model. Softw. 59, 98–108.

De Louw, P.G.B., Eeman, S., Oude Essink, G.H.P., Vermue, E., Post, V.E.A., 2013. Rainwater lens dynamics and mixing between infiltrating rainwater and upward saline groundwater seepage beneath a tile-drained agricultural field. J. Hydrol. 501, 133–145.

De Louw, P.G.B., Eeman, S., Siemon, B., Voortman, B.R., Gunnink, J.L., van Baaren, E.S., Oude Essink, G.H.P., 2011a. Shallow rainwater lenses in deltaic areas with saline seepage. Hydrol. Earth Syst. Sci. 15, 3659–3678.

De Louw, P.G.B., Van der Velde, Y., Van der Zee, S.E.A.T.M., 2011b. Quantifying water and salt fluxes in a lowland polder catchment dominated by boil seepage: a probabilistic end-member mixing approach. Hydrol. Earth Syst. Sci. 15, 2101–2117.

Delsman, J.R., 2015. Saline groundwater - Surface Water Interaction in Coastal Lowlands. PhD thesis. VU University Amsterdam.

Delsman, J.R., Hu-a-ng, K.R.M., Vos, P.C., De Louw, P.G.B., Oude Essink, G.H.P., Stuyfzand, P.J., Bierkens, M.F.P., 2014a. Paleo-modeling of coastal saltwater intrusion during the Holocene: an application to The Netherlands. Hydrol. Earth Syst. Sci. 18, 3891–3905.

Delsman, J.R., Waterloo, M.J., Groen, M.M.A., Groen, J., Stuyfzand, P.J., 2014b. Investigating summer flow paths in a Dutch agricultural field using high frequency direct measurements. J. Hydrol. 519, 3069–3085.

Delsman, J.R., Winters, P., Vandenbohede, A., Oude Essink, G.H.P., Lebbe, L., 2016. Global sampling to assess the value of diverse observations in conditioning a real-world groundwater flow and transport model. Water Resour. Res. 52, 1652–1672.

Devos, J., Raats, P.A.C., Feddes, R., 2002. Chloride transport in a recently reclaimed Dutch polder. J. Hydrol. 257, 59–77.

Eeman, S., Leijnse, A., Raats, P.A.C., Van der Zee, S.E.A.T.M., 2011. Analysis of the thickness of a fresh water lens and of the transition zone between this lens and upwelling saline water. Adv. Water Resour. 34, 291–302.

Eeman, S., Van der Zee, S.E.A.T.M., Leijnse, A., De Louw, P.G.B., Maas, C., 2012. Response to recharge variation of thin rainwater lenses and their mixing zone with underlying saline groundwater. Hydrol. Earth Syst. Sci. 16, 3535–3549.

Ernst, L., 1973. De bepaling van de transporttijd van het grondwater bij stroming in de verzadigde zone [in Dutch]. ICW Nota 755. ICW Nota, Wageningen, Netherlands.

Ferguson, G., Gleeson, T., 2012. Vulnerability of coastal aquifers to groundwater use and climate change. Nat. Clim. Chang. 2, 342–345.

Forzieri, G., Feyen, L., Rojas, R., Flörke, M., Wimmer, F., Bianchi, a., 2014. Ensemble projections of future streamflow droughts in Europe. Hydrol. Earth Syst. Sci. 18, 85–108.

Groenendijk, P., Renaud, L., Roelsma, J., 2005. Prediction of Nitrogen and Phosphorus Leaching to Groundwater and Surface Waters - Process Descriptions of the animo4.0 Model, Alterra Report. Alterra Wageningen UR, Wageningen, Netherlands.

Groenendijk, P., Van den Eertwegh, G.A.P.H., 2004. Drainage-water travel times as a key factor for surface water contamination. In: Unsaturated-zone Modeling: Progress, Challenges and Applications. Kluwer Academic Pub, p. 145.

Haasnoot, M., van Deursen, W.P.A., Guillaume, J.H.A., Kwakkel, J.H., van Beek, E., Middelkoop, H., 2014. Fit for purpose? Building and evaluating a fast, integrated model for exploring water policy pathways. Environ. Model. Softw. 60, 99–120.

Hooghoudt, S.B., 1940. Bijdrage tot de kennis van enige natuurkundige grootheden van den grond, Deel 7. Versl. van Landbouwkd. Onderz 46, 515–707.

Iorgulescu, I., Beven, K.J., Musy, a., 2005. Data-based modelling of runoff and chemical tracer concentrations in the Haute-Mentue research catchment (Switzerland). Hydrol. Process 19, 2557–2573.

IPCC, 2013. Summary for policymakers. In: Stocker, T.F., Qin, D., Plattner, G.-K., Tignor, M., Allen, S.K., Boschung, J., Nauels, A., Xia, Y., Bex, V., Midgley, P.M. (Eds.), Climate Change 2013: the Physical Science Basis. Contribution of Working Group I to the Fifth Assessment Report of the Intergovernmental Panel on Climate Change. Cambridge University Press, Cambridge, UK and New York, NY, USA, p. 28.

Jury, W., Vaux, H., 2005. The role of science in solving the world's emerging water problems. Proc. Natl. Acad. Sci. U. S. A. 102, 15715–15720.

Kirchner, J.W., 2006. Getting the right answers for the right reasons: linking measurements, analyses, and models to advance the science of hydrology. Water Resour. Res. 42, 1–5.

Kroes, J.G., van Dam, J.C., Groenendijk, P., Hendriks, R.F.A., Jacobs, C.M.J., 2008. SWAP Version 3.2: Theory Description and User Manual, Alterra Report. Alterra Wageningen UR, Wageningen, Netherlands.

Langevin, C.D., Thorne Jr., D.T., Dausman, A.M., Sukop, M.C., Guo, W., 2008. SEAWAT Version 4: a Computer Program for Simulation of Multi-species Solute and Heat Transport, Methods. U.S. Geological Survey, Reston, Virginia.

Maas, C., 2007. Influence of climate change on a Ghijben–Herzberg lens. J. Hydrol. 347, 223–228.

Mantovan, P., Todini, E., 2006. Hydrological forecasting uncertainty assessment: incoherence of the GLUE methodology. J. Hydrol. 330, 368–381.

McDonnell, J.J., Beven, K.J., 2014. Debates on Water Resources: the future of hydrological sciences: a (common) path forward? A call to action aimed at understanding velocities, celerities and residence time distributions of the headwater hydrograph. Water Resour. Res. 50, 1–9.

McLeod, M.K., Slavich, P.G., Irhas, Y., Moore, N., Rachman, a., Ali, N., Iskandar, T., Hunt, C., Caniago, C., 2010. Soil salinity in aceh after the december 2004 indian ocean tsunami. Agric. Water Manag. 97, 605–613.

Moody, W.T., 1966. Nonlinear differential equation of drain spacing. J. Irrig. Drain. Div. Amer. Soc. Civ. Eng. 92, 1–9.

Oude Essink, G.H.P., Van Baaren, E.S., De Louw, P.G.B., 2010. Effects of climate change on coastal groundwater systems: a modeling study in the Netherlands. Water Resour. Res. 46, 1–16.

Post, V.E.A., Groen, J., Kooi, H., Person, M., Ge, S., Edmunds, W.M., 2013. Offshore fresh groundwater reserves as a global phenomenon. Nature 504, 71–78.

Post, V.E.A., Plicht, H., Meijer, H., 2003. The origin of brackish and saline groundwater in the coastal area of the Netherlands. Netherl. Geosci./Geol. Mijnb 82, 133–147.

Quinn, N.W.T., Brekke, L.D., Miller, N.L., Heinzer, T., Hidalgo, H., Dracup, J.A., 2004. Model integration for assessing future hydroclimate impacts on water resources, agricultural production and environmental quality in the San Joaquin Basin, California. Environ. Model. Softw. 19, 305–316.

Rojas, R., Feyen, L., Batelaan, O., Dassargues, A., 2010. On the value of conditioning data to reduce conceptual model uncertainty in groundwater modeling. Water Resour. Res. 46, W08520.

Smedema, L., Poelman, A., De, Haan, W., 1985. Use of the Hooghoudt formula for drain spacing calculations in homogeneous-anisotropic soils. Agric. water Manag. 10, 283–291.

Stedinger, J.R., Vogel, R.M., Lee, S.U., Batchelder, R., 2008. Appraisal of the generalized likelihood uncertainty estimation (GLUE) method. Water Resour. Res. 44, W00B06.

Therrien, R., Mclaren, R.G., Sudicky, E.A., Panday, S.M., 2010. HydroGeoSphere a Three-dimensional Numerical Model Describing Fully-integrated Subsurface and Surface Flow and Solute Transport, Groundwater Simulations Group. University of Waterloo, Waterloo, ON.

van Dam, J.C., Groenendijk, P., Hendriks, R.F.A., Kroes, J.G., 2008. Advances of modeling water flow in variably saturated soils with SWAP. Vadose Zo. J. 7, 640.

Van der Velde, Y., De Rooij, G.H., Rozemeijer, J.C., Van Geer, F.C., Broers, H.P., 2010. Nitrate response of a lowland catchment: on the relation between stream concentration and travel time distribution dynamics. Water Resour. Res. 46, 1–17.

Van der Velde, Y., Torfs, P.J.J.F., Van der Zee, S.E.A.T.M., Uijlenhoet, R., 2012.

Quantifying catchment-scale mixing and its effect on time-varying travel time distributions. Water Resour. Res. 48, 1–13.
van Turnhout, A.G., Kleerebezem, R., Heimovaara, T.J., 2016. A toolbox to find the best mechanistic model to predict the behavior of environmental systems. Environ. Model. Softw. 83, 344–355.
Vandenbohede, A., Mollema, P.N., Greggio, N., Antonellini, M., 2014. Seasonal dynamic of a shallow freshwater lens due to irrigation in the coastal plain of Ravenna, Italy. Hydrogeol. J. 281.
Velstra, J., Groen, J., De Jong, K., 2011. Observations of salinity patterns in shallow groundwater and drainage water from agricultural land in the northern part of the Netherlands. Irrig. Drain. 60, 51–58.
Verhoeven, G., Harezlak, V., Oude Essink, G.H.P., 2013. Zoetwateraanvoer Tholen [in Dutch], Deltares rapport 1202277. Delft, Netherlands.
Voss, C.I., 2011. Groundwater modeling fantasies —part 1, adrift in the details. In: 's message (Ed.), Hydrogeol. J. vol. 19, 1281–1284.
Wada, Y., van Beek, L.P.H., Wanders, N., Bierkens, M.F.P., 2013. Human water consumption intensifies hydrological drought worldwide. Environ. Res. Lett. 8, 034036.
Wagener, T., Boyle, D., Lees, M.J., Wheater, H.S., Gupta, H.V., Sorooshian, S., 2001. A framework for development and application of hydrological models. Hydrol. Earth Syst. Sci. 5, 13–26.
Werner, A.D., Bakker, M.A.J., Post, V.E.A., Vandenbohede, A., Lu, C., Ataie-Ashtiani, B., Simmons, C.T., Barry, D.A., 2013. Seawater intrusion processes, investigation and management: recent advances and future challenges. Adv. Water Resour. 51, 3–26.
Yu, P.-S., Yang, T.-C., Chen, S.-J., 2001. Comparison of uncertainty analysis methods for a distributed rainfall–runoff model. J. Hydrol. 244, 43–59.
Zheng, C., 2009. Recent developments and future directions for MT3DMS and related transport codes. Ground Water 47, 620–625.
Zheng, C., Wang, P., 1999. MT3DMS: a Modular Three-dimensional Multispecies Transport Model for Simulation of Advection, Dispersion, and Chemical Reactions of Contaminants in Groundwater Systems; Documentation and User's Guide. Washington, DC.
Zhou, H., Gómez-Hernández, J.J., Li, L., 2014. Inverse methods in hydrogeology: evolution and recent trends. Adv. Water Resour. 63, 22–37.